Supplement of Solid Earth, 5, 1169–1188, 2014
http://www.solid-earth.net/5/1169/2014/
doi:10.5194/se-5-1169-2014-supplement

Solid Earth
Open Access

Supplement of

Wave-equation-based travel-time seismic tomography – Part 2: Application to the 1992 Landers earthquake (M_w 7.3) area

P. Tong et al.

Correspondence to: P. Tong (tongping85@gmail.com)

1 Checkerboard resolution tests

To further reveal the ability of WETST in recovering heterogeneous structures, we continue to conduct checkerboard resolution tests by adding noise to the data. To account for the picking errors as existing in the real data, we add random errors with a standard deviation of 0.1 s for *P*-wave and a standard deviation of 0.18 s for *S*-wave to the synthetic arrival times. Figs. S1-S2 show the results of the checkerboard tests at six layers for the Vp and Vs structures, respectively. Comparison between the results shown in Figs. 8a-e and Figs. 9a-e and the inversion results in Figs. S1-S2 generated with random errors shows that the picking errors have very limited influence on the final tomographic results.

2 Poisson ratio's structure

The generally well recovered V_p and V_s structures in our checkerboard resolution tests imply that a reliable Poisson's ratio structures can be derived from this tomographic study. In this section, we demonstrate the map views of the iteratively updated Poisson's ratio models as in Figs. S3-S5.

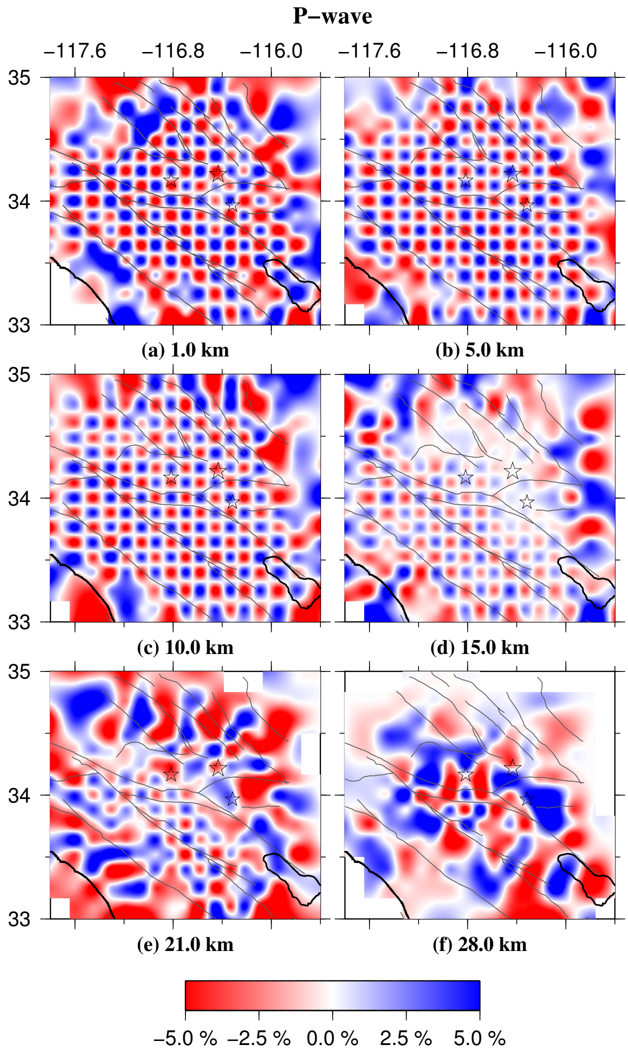

P−wave
−117.6
−116.8
−116.0
35
34
33
(a) 1.0 km
(b) 5.0 km
(c) 10.0 km
(d) 15.0 km
(e) 21.0 km
(f) 28.0 km
−5.0 %
−2.5 %
0.0 %
2.5 %
5.0 %

Figure S1. *P*-wave checkerboard resolution test with the whole chosen data set in this study. Random errors with a standard deviation of 0.1 s were added to the arrival-times.

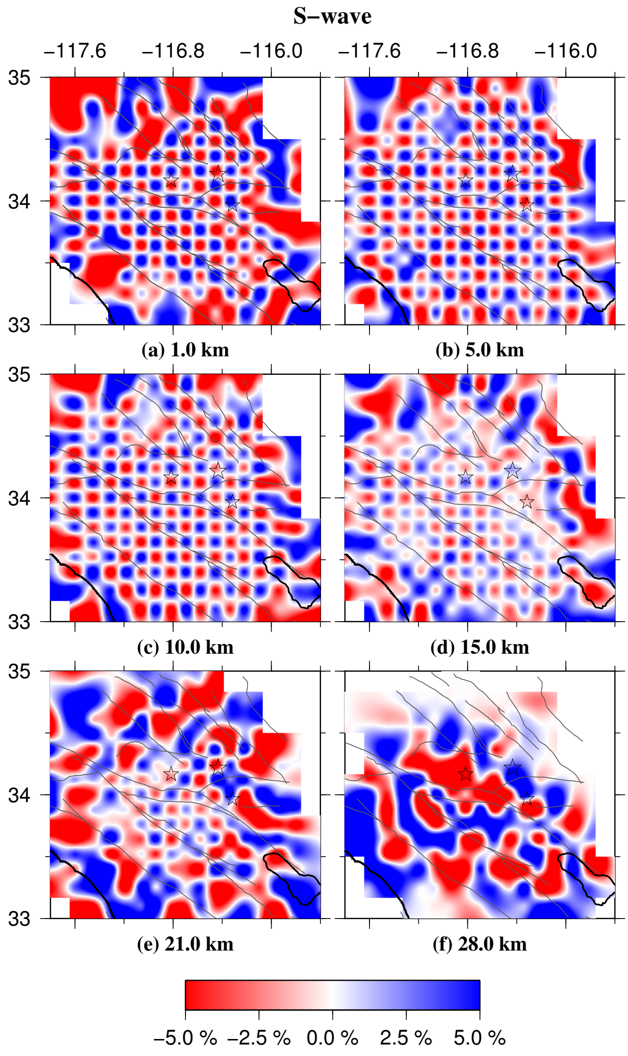

S−wave
−117.6
−116.8
−116.0
35
34
33
(a) 1.0 km
(b) 5.0 km
(c) 10.0 km
(d) 15.0 km
(e) 21.0 km
(f) 28.0 km
−5.0 %
−2.5 %
0.0 %
2.5 %
5.0 %

Figure S2. *S*-wave checkerboard resolution test with the whole chosen data set in this study. Random errors with a standard deviation of 0.18 s were added to the arrival-times.

Poisson's ratio (Model 2)

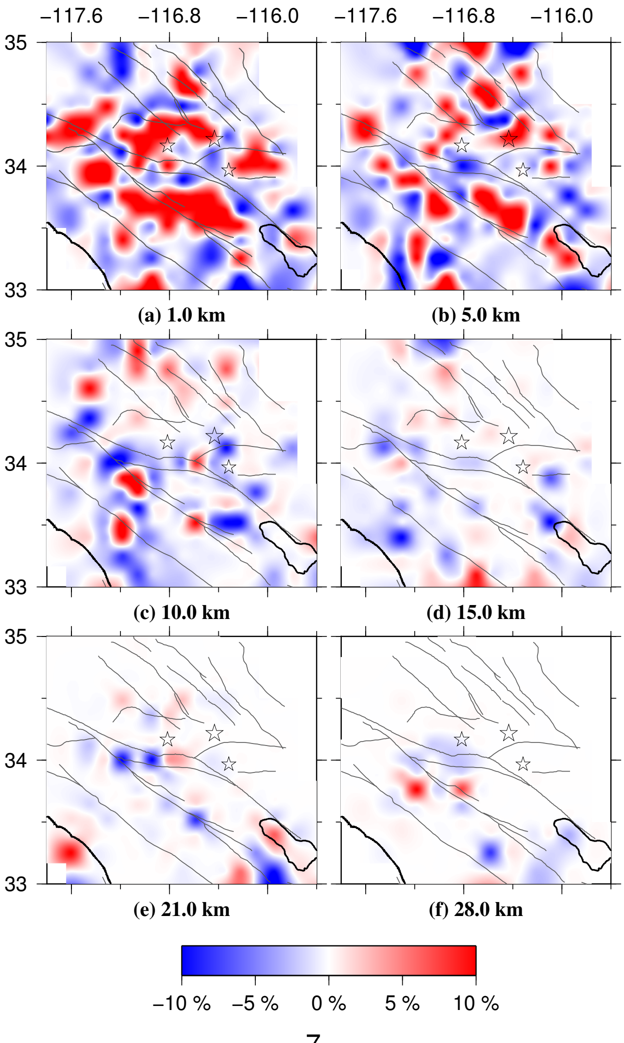

Figure S3. Map views of the Poisson's ratio structure at six representative depths for m_2 obtained at the first iteration. The layer depth is shown just on the right hand side of each row. Red and blue colours denote high and low Poisson's ratio, respectively. The Poisson's ratio perturbation scale (in per cent) is also shown. On each map, grey lines denote active faults.

Poisson's ratio (Model 3)

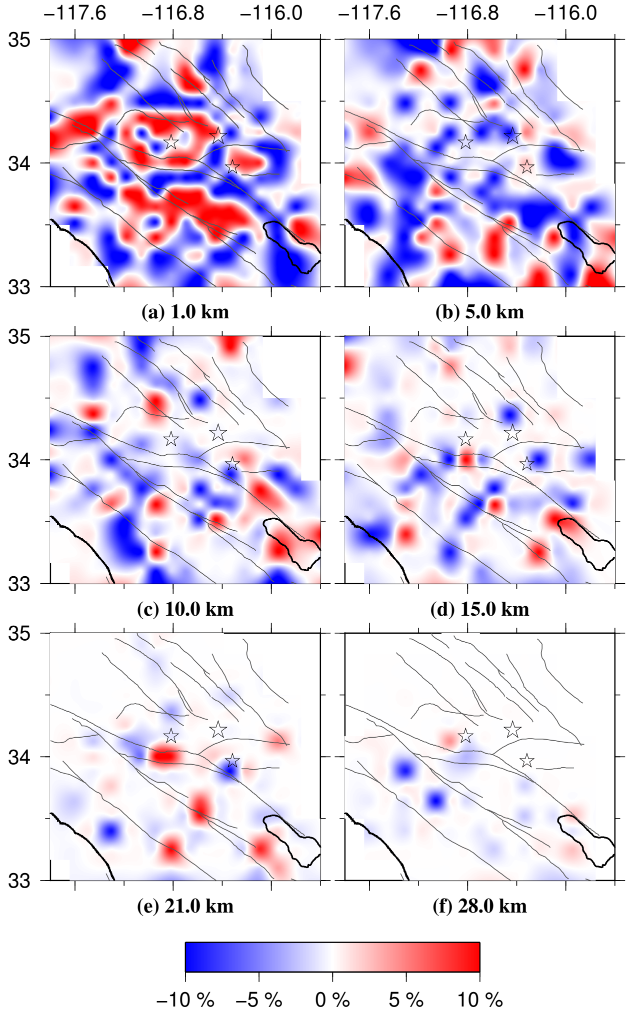

Figure S4. The same as Fig. S3 but for m_3 obtained at the second iteration.

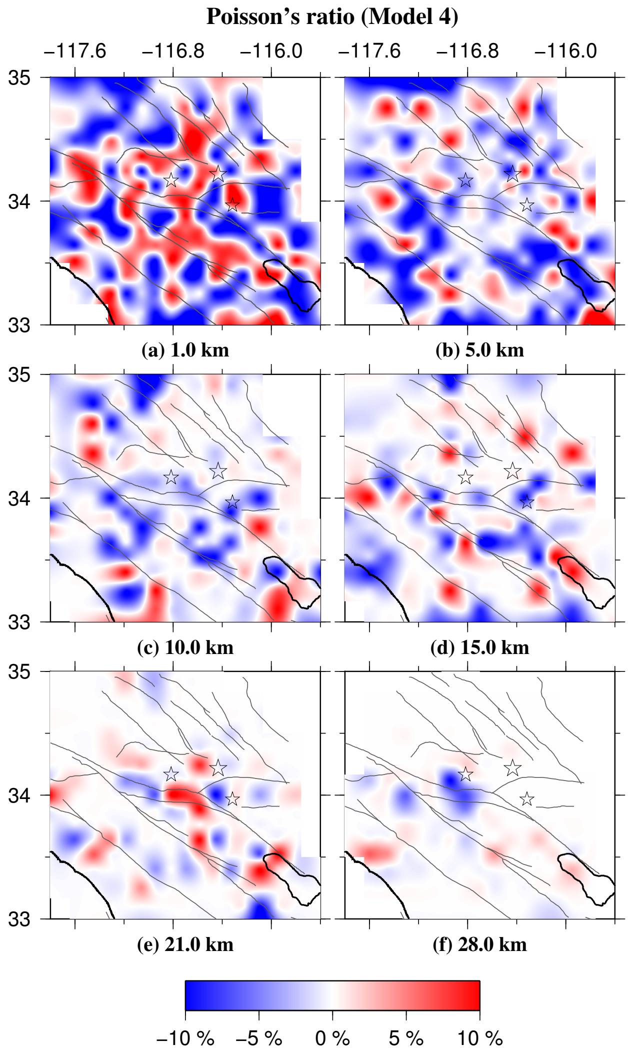
Poisson's ratio (Model 4)
−117.6
−116.8
−116.0
35
34
33
(a) 1.0 km
(b) 5.0 km
(c) 10.0 km
(d) 15.0 km
(e) 21.0 km
(f) 28.0 km
−10 %
−5 %
0 %
5 %
10 %

Figure S5. The same as Fig. S3 but for m_4, the final model.